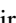



Orbital-dependent electric field effect on magnetism in ultrathin cobaltKihiro T. Yamada ^{1,2,*} Yoichi Shiota ¹ Tomohiro Koyama,^{3,4} Yoshinori Kotani,⁵ Kentaro Toyoki,⁵ Hayato Mizuno,¹ Fuyuki Ando,¹ Kohji Nakamura,⁶ Tetsuya Nakamura,⁵ Daichi Chiba,^{3,4} and Teruo Ono^{1,4,†}¹*Institute for Chemical Research, Kyoto University, Uji, Kyoto 611-0011, Japan*²*Department of Physics, Tokyo Institute of Technology, Tokyo 152-8551, Japan*³*The Institute of Scientific and Industrial Research, Osaka University, Ibaraki 567-0047, Japan*⁴*Center for Spintronics Research Network (CSRN), Graduate School of Engineering Science, Osaka University Ibaraki 560-8531, Japan*⁵*Japan Synchrotron Radiation Research Institute, Sayo, Hyogo 679-5198, Japan*⁶*Graduate School of Engineering, Mie University, Tsu, Mie 514-8507, Japan*

(Received 4 September 2019; accepted 13 August 2020; published 17 September 2020)

Electric field modulations of magnetism in ferromagnetic metals are in general ascribed to the electric field effects on the orbitals. However, a direct observation of the electric-field-induced changes in the orbital states of a ferromagnetic metal is lacking. In this Rapid Communication, we demonstrate that an electric field applied to an ultrathin Co film can change the electron occupations according to the orbitals, combining x-ray absorption and x-ray magnetic circularly dichroism spectroscopies with the sum rules. Under a positive electric field, the $d_{xz(yz)}$ -occupied states decrease mainly via the modification of orbital hybridizations, while the d_{z^2} -occupied state increases. The changes in the d_{xz} and d_{yz} states dominantly alter the Curie temperature.

DOI: [10.1103/PhysRevB.102.100407](https://doi.org/10.1103/PhysRevB.102.100407)

The diverse range of phenomena in condensed matter systems originates from the orbital degree of freedom in concert with the spin and charge degrees of freedom. In strongly correlated oxides, for instance, exotic phenomena including metal-insulator transitions, high-temperature superconductivity, and colossal magnetoresistance emerge as a consequence of the synergy of the three ingredients [1]. As for thin ferromagnetic metals, it has been known for decades that the magnetic anisotropy arises microscopically from the anisotropic distribution of the orbital moment connected to the spin via the spin-orbit interaction [2]. Modern-day spintronics actively uses the orbital degree of freedom together with the spin and charge degrees of freedom [3,4], leading to remarkable developments in the spin-orbit torque [5] and the interfacial Dzyaloshinskii-Moriya interaction [6] in ferromagnetic metal/heavy metal heterostructures. In addition to the interesting physics, such phenomena are crucial to the ultrafast and energy-efficient operation of next-generation magnetic-recording devices [7]. Therefore, exploring ways to control the orbital degree of freedom is increasingly becoming important as one of the possible future directions in fundamental as well as applied fields.

An electric field can modify the spatial electron distributions of condensed matter, thus enabling the control of the electronic as well as magnetic properties [8,9]. Electric field control of magnetic anisotropy [10–12] and the phase transition [13] have been realized in ultrathin Fe and Co ferromagnetic metals. Electric-field-induced magnetization switching in ferromagnetic systems [14,15] with a large thermal stability

has drawn much attention from the industry as an ultraefficient magnetic-recording technique [16]. Such electric field effects on magnetism in ferromagnetic metals are, in general, attributed to the modified orbitals. However, the electric field effect on the orbitals and its connection to the modulation of magnetic properties still needs to be investigated.

In this Rapid Communication, we demonstrate that the application of an electric field to an ultrathin cobalt film can modify the electron occupations according to the orbitals. The orbital-dependent electric field effect microscopically brings about a change in the Curie temperature (T_C). To study the electric-field-induced orbital-dependent changes in the $3d$ holes, i.e., the unoccupied $3d$ states, we employed x-ray magnetic circularly T_C dichroism (XMCD) and absorption spectroscopy (XAS) [17–20] techniques on the basis of sum rules [21–23]. The microscopic study enabled us to prove that the positive (negative) electric field decreases (increases) the d_{z^2} holes but increased (decreased) the $d_{xz(yz)}$ holes. This result is considered to have been derived not only from the electric-field-induced shift of the Fermi level but also from the changes in orbital hybridizations. Furthermore, we correlated the change in T_C with the electric-field-induced changes in the $3d$ holes, to reveal the entangled mechanism. The change in T_C is considered to be ruled by the changes in the $d_{xz(yz)}$ states, because they have stronger ferromagnetic exchange interactions than the d_{z^2} states.

We fabricated capacitors consisting of Ta(5 nm)/Pt(10 nm)/HfO₂(50 nm)/MgO(2 nm)/Co(0.44 nm)/Pt(3 nm) on a semi-insulated GaAs substrate by using standard photolithography techniques. The sputter-deposited MgO layer on the amorphous layer HfO₂ will be (001) oriented [24], because the surface energy of the (001) plane is much smaller than the other major crystal planes [25]. The ultrathin

*Corresponding author: yamada@phys.titech.ac.jp†Corresponding author: ono@scl.kyoto-u.ac.jp

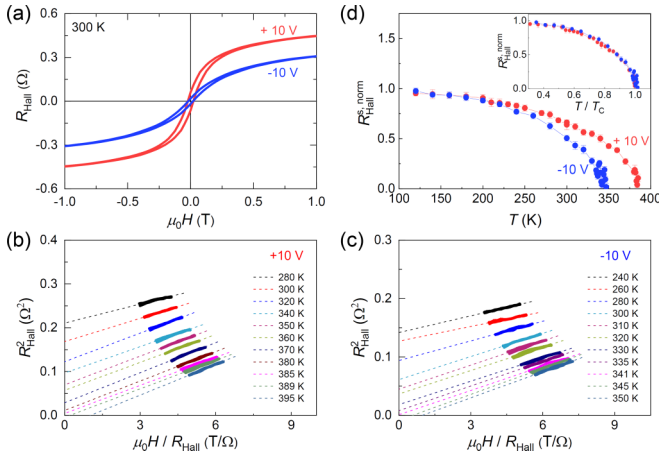


FIG. 1. (a) Hall-resistance (R_{Hall}) curves under gate voltages (V_G) of ± 10 V at temperatures (T) of 300 K. R_{Hall} was measured while sweeping a magnetic (H) in the perpendicular direction to the device surface. (b) and (c) Arrott plots for $V_G = \pm 10$ V. The dashed curves display linear fitting to data points, measured at high magnetic fields (> 1.5 T). (d) Normalized saturation Hall resistances ($R_{\text{Hall}}^{s, \text{norm}}$) as a function of T . The saturation values of R_{Hall} were obtained from the y intercept of the Arrott plot. The inset indicates $R_{\text{Hall}}^{s, \text{norm}}$ as a function of T rescaled by the Curie temperature (T_C).

Co layer would not be contiguous, but the fcc [001] axis of each island tends to be oriented parallel to the MgO [001] axis [26]. The Co/Pt top electrode was shaped into Hall-bar and square patterns, respectively, for electrical-transport and x-ray measurements. See Supplemental Material (SM) Note 1 [27] for details of the fabrication process. Here, the application of a positive (negative) gate voltage V_G between the two electrodes increases (decreases) the electron density of the MgO/Co surface.

We performed magnetotransport measurements to investigate the electric-field-induced changes in the T_C of the Co thin film. See SM Note 2 [27] for the detailed measurement conditions. Figure 1(a) shows the perpendicular magnetic field (H) dependence of Hall resistance (R_{Hall}) at 300 and 340 K and a V_G of ± 10 V (± 1.92 MV/cm). Here, R_{Hall} is generated from the anomalous Hall effect, where R_{Hall} is proportional to the perpendicular component of magnetization. In the Pt/Co/MgO structures, the temperature dependence of R_{Hall} approximately coincides with that of the magnetization [13]. At both temperatures, R_{Hall} increases (decreases) by the application of a V_G of $+10$ (-10) V. This is mostly due to the increase (decrease) in magnetization of the Co layer.

To accurately determine the T_C at each V_G , the Arrott plot technique was used [28]. R_{Hall}^2 was plotted as a function of H/R_{Hall} , as shown in Figs. 1(b) and 1(c). The intercept of the linear fitting of high-magnetic-field data points corresponds to the square of the saturation value of R_{Hall} , and becomes zero at T_C . From the zero intercept, the values of T_C are determined to be 385 and 341 K at $V_G = +10$ and -10 V, respectively; thus, the change in T_C is 44 K. This T_C change corresponds to the variation in exchange stiffness of 0.66 meV 2 , using the linear relationship [29] between the electric-field-induced changes in T_C and those in the exchange interaction in a stack similar to the present system.

To clarify the shift, Fig. 1(d) shows the saturation values of the Hall resistance ($R_{\text{Hall}}^{s, \text{norm}}$) normalized with that at 10 K as a function of T . By scaling $R_{\text{Hall}}^{s, \text{norm}}$ with the normalized temperature (T/T_C), the two rescaled curves coincide with each other [see the inset of Fig. 1(d)]. This indicates that the large changes observed in R_{Hall} result from the change in T_C . The observed change in T_C is twice as large as those in the systems with reversed stacking MgO/Co/Pt [13]. A plausible explanation for this observation is that the Co lattice is distorted by the MgO underlayer [30]. For instance, in a Ta/Pt/Co/Pd stack on a GaAs substrate, distortions induced in the magnetic layer by the substrate can enhance the electric field modulation of the magnetic anisotropy [31].

To observe the orbital-dependent electric field effect on the electron occupation, we used the partial fluorescence yield method [32] of the BL25SU at the SPring-8 facility to measure the XAS and XMCD intensities around the Co $L_{2,3}$ edge of ultrathin cobalt under a V_G . The magnetization was saturated in the direction of a magnetic field (H) of 1.9 T applied at the angle (θ) of 20° or 70° from the device's normal. The x ray was circularly polarized by twin helical undulators and incident onto the device, which was tilted at 10° to the direction of the magnetic field [32]. Because the system has a relatively small effective magnetic anisotropy field [0.17 (-0.05) T at $V_G = +10$ (-10) V at 300 K [27]], the magnetization was saturated in the magnetic field direction under all the measurement conditions. The x-ray fluorescence generated from the Co atoms was measured by a multielement silicon-drift detector at room temperature. See SM Note 3 for further details of the x-ray measurements [27].

Figures 2(a) and 2(b) respectively show the XAS intensity I_{XAS} at $V_G = \pm 10$ V together with the difference spectra between $V_G = +10$ and -10 V, $\Delta I_{\text{XAS}} = I_{\text{XAS}}(+10 \text{ V}) - I_{\text{XAS}}(-10 \text{ V})$, at $\theta = 20^\circ$ and 70° . The negative V_G increases the intensities around the L_3 and L_2 absorption edges for both the angles. This means that the total number of $3d$ holes of Co (h_t) decreases (increases) by applying $V_G = +10$ (-10) V. When switching V_G from $+10$ to -10 V, h_t increases by 0.045 ± 0.001 (0.034 ± 0.001) holes per Co atom for $\theta = 20^\circ$ (70°). The small angular dependence of h_t may be due to the self-absorption effect [33]. The variation in h_t is larger than that expected from the capacitance [34], 0.011 [27]. A plausible explanation for this is that the band structure of the Co layer was modified by introducing the electric field, as discussed later. Satellite peaks of oxidized Co [35] were not found around the main peaks of Co (for further details, see SM Note 7 [27]). This means that the observed changes by V_G are dominated not by electrochemical reactions [36–38] but by electrostatic charge accumulations, as also demonstrated by the x-ray photoelectron spectroscopies [39].

Figures 2(c) and 2(d) show the XMCD intensities (I_{XMCD}) at $V_G = \pm 10$ V and their differences, $\Delta I_{\text{XMCD}} = I_{\text{XMCD}}(+10 \text{ V}) - I_{\text{XMCD}}(-10 \text{ V})$, at $\theta = 20^\circ$ and 70° , respectively. I_{XMCD} at $\theta = 20^\circ$ shows a meaningful change [Fig. 2(c)], whereas I_{XMCD} at $\theta = 70^\circ$ shows no change [Fig. 2(d)]. These changes in the spectra are reproducible (see SM Note 8 [27]). Subsequently, we applied the sum rules to the integrated values of I_{XAS} and I_{XMCD} to evaluate the values of the effective spin moment m_{eff} and orbital magnetic moment m_L (for details of the sum-rule analysis, see SM

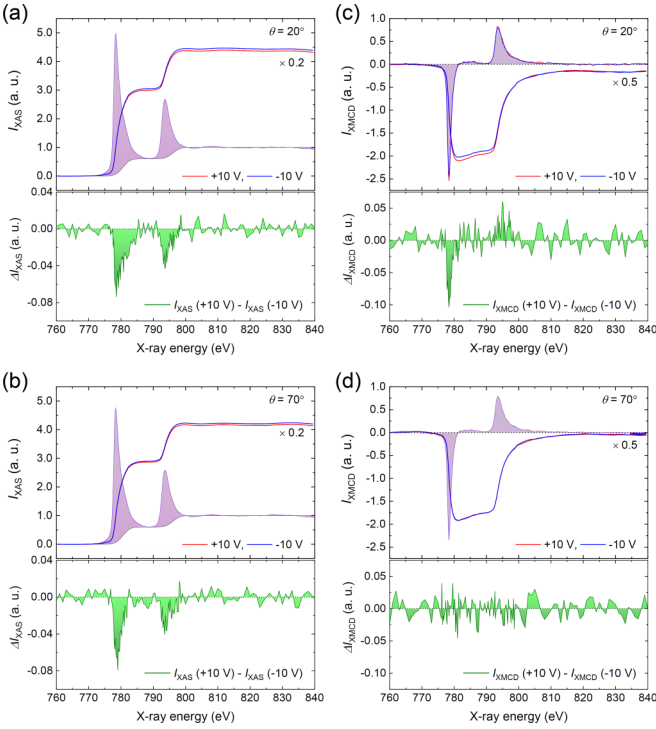


FIG. 2. XAS intensities (I_{XAS}) under V_G of ± 10 V and their differences (ΔI_{XAS}) measured at magnetic field angles (θ) of (a) 20° and (b) 70° . The black lines show double-step functions with a step ratio of 2:1, which were used to remove the contribution of the nonresonant absorptions. XMCD intensities under $V_G = \pm 10$ V and their difference (ΔI_{XMCD}), measured at (c) $\theta = 20^\circ$ and (d) 70° . The integration curves of I_{XAS} and I_{XMCD} , multiplied by factors of 0.2 and 0.5, were plotted together with I_{XAS} and I_{XMCD} , respectively.

Note 4 [27]). Table I summarizes the evaluated values of magnetic moments per Co atom. The perpendicular [m_L^\perp ($\theta = 0^\circ$)] and in-plane [m_L^\parallel ($\theta = 90^\circ$)] components of m_L were estimated from the two values of m_o determined at two different angles ($\theta = 20^\circ$ and 70°) using the relation [23,40] $m_L^o = m_L^\perp \cos^2\theta + m_L^\parallel \sin^2\theta$. Moreover, we determined m_s as well as the perpendicular (m_{eff}^\perp) and in-plane (m_{eff}^\parallel) components of m_{eff} from the two values of m_{eff} at the two angles, using the angular dependence of the magnetic dipole moment [23,41,42], $m_T \propto (3\cos^2\theta - 1)$. m_{eff}^\perp is significantly changed by V_G , in contrast to m_{eff}^\parallel that underwent no meaningful change. The spin magnetic moment (m_s) increases by the elevation of T_C at $V_G = +10$ V. We could not observe any meaningful changes in $\Delta m_L = m_L^\perp - m_L^\parallel$ with the current measurement accuracy.

The terms m_{eff}^\perp and m_{eff}^\parallel are sensitive to spin magnetic moments ($m_{s,i}$) projected to the different d orbitals ($i = d_{z^2}, d_{xz}, d_{yz}, d_{xy},$ or $d_{x^2-y^2}$), as the system satisfies the following conditions [17,23,42]. First, the spin-orbit interaction is much smaller than the exchange splitting [2,23]. Second, the symmetry of the present system is considered to be higher than D_{2h} . When the magnetization and wave vector of the circularly polarized x-ray beam are aligned in the z and $x(y)$ axes of a Co crystal, the z and $x(y)$ components of m_{eff} are given by $m_{\text{eff}}^z = -m_{s,d_{z^2}} + 3m_{s,d_{x^2-y^2}} + 3m_{s,d_{xy}}$ and $m_{\text{eff}}^{x(y)} =$

TABLE I. Magnetic moments and hole number of Co estimated using the sum rules. m_{eff} , m_s , m_T , and m_L denote the effective spin magnetic moment, spin magnetic moment, magnetic dipole moment, and orbital magnetic moment at a magnetic angle in the units of μ_B (Bohr magneton) per Co atom, respectively. h_i represents the $3d$ hole number per Co atom determined from the XAS intensities.

	θ	$V_G = \pm 10$ V	$V_G = -10$ V
m_{eff}	0°	1.497 ± 0.004	1.425 ± 0.003
	20°	1.469 ± 0.002	1.407 ± 0.001
	70°	1.285 ± 0.003	1.288 ± 0.002
	90°	1.257 ± 0.003	1.270 ± 0.002
m_s	0°	1.337 ± 0.002	1.322 ± 0.001
	90°	0.160 ± 0.003	0.103 ± 0.002
$-7m_T$	0°	0.125 ± 0.001	0.123 ± 0.001
	20°	0.121 ± 0.001	0.119 ± 0.001
m_L	70°	0.090 ± 0.001	0.090 ± 0.001
	90°	0.085 ± 0.001	0.086 ± 0.001
	20°	2.778 ± 0.001	2.823 ± 0.001
h_i	70°	2.481 ± 0.001	2.515 ± 0.001

$2m_{s,d_{z^2}} + 3m_{s,d_{xz(xz)}}$, respectively. Here, m_{eff}^z is identical to m_{eff}^\perp . The average of m_{eff}^x and m_{eff}^y corresponds to m_{eff}^\parallel because the in-plane orientations of Co islands are not be aligned. See SM Note 5 [27] and Ref. [23] for more details of this analysis.

To discuss the changes in the hole (h_i) of the specific d -orbital state, we assumed that the variations of $m_{s,i}$ by V_G could be ascribed only to those of the $3d$ holes in the minority-spin band. This can be a good approximation because the $3d$ majority-spin band of Co on Pt is almost wholly occupied [43] (i.e., the hole in the majority band is ~ 0). This enabled us to estimate the contribution of the hole ($h^{\perp(\parallel)}$) to the $m_{\text{eff}}^{\perp(\parallel)}$ as follows: $h^\perp = m_{\text{eff}}^\perp / (m_s / h_i) = -h_{d_{z^2}} + 3(h_{d_{x^2-y^2}} + h_{d_{xy}})$ and $h^\parallel = m_{\text{eff}}^\parallel / (m_s / h_i) = 2h_{d_{z^2}} + \frac{3}{2}(h_{d_{xz}} + h_{d_{yz}})$. Furthermore, we estimated the variation of the hole of a specific d -orbital state, $\Delta h_i = h_i(+10 \text{ V}) - h_i(-10 \text{ V})$. Using the values in Table I, the variations of h^\perp and h^\parallel were estimated to be $\Delta h^\perp = 3(\Delta h_{d_{x^2-y^2}} + \Delta h_{d_{xy}}) - \Delta h_{d_{z^2}} = 0.067 \pm 0.016$ and $\Delta h^\parallel = 2\Delta h_{d_{z^2}} + \frac{3}{2}(\Delta h_{d_{xz}} + \Delta h_{d_{yz}}) = -0.084 \pm 0.008$, respectively. The summation of these two relations gives the total change in the $3d$ holes: $(\Delta h^\perp + 2\Delta h^\parallel)/3 = \Delta h_{d_{z^2}} + \Delta h_{d_{xz}} + \Delta h_{d_{yz}} + \Delta h_{d_{x^2-y^2}} + \Delta h_{d_{xy}} = -0.034 \pm 0.008$. This value agrees with the variation of h_i estimated solely from the XAS intensity. Because the wave functions of the $d_{x^2-y^2}$ and d_{xy} orbitals are distributed in the film plane, the occupations are probably much less affected by the electric field perpendicular to the film plane than those of the d_{z^2} states [44]. Hence, assuming $\Delta h_{d_{x^2-y^2}} + \Delta h_{d_{xy}} \sim 0$ in the Δh^\perp relation, we obtain $\Delta h_{d_{z^2}} \sim -0.067$. Substituting $\Delta h_{d_{z^2}} \sim -0.067$ into the Δh^\parallel relation, we obtain $\Delta h_{d_{xz}} + \Delta h_{d_{yz}} \sim 0.033$. In other words, the positive electric field injects electrons into the d_{z^2} states but extracts electrons from the d_{xz} and d_{yz} states. One can find similar trends in the theoretical calculations using Fe/Pt/MgO [45] and V/Fe/Co/MgO [46], even though they do not make reference to this point. Therefore, the observed

trend should be expected in other oxide/ferromagnetic metal heterostructures.

It is well known that the values of the spin magnetic moment [47,48] and T_C [49] of a series of bulk ferromagnetic transition metals are described as a function of the number of $3d$ electrons. In the Slater-Pauling curve, the spin magnetic moment and T_C of Co decreases with increasing $3d$ electron occupations (i.e., with decreasing $3d$ holes). On the other hand, this trend is reversed in bulk Fe. The well-established relation in bulk metals holds true even in ultrathin films [50], and is anticipated to account for the electric field modulation of T_C . However, previous studies on the electric field effect on T_C in ultrathin cobalt films [13,29] appear to reveal trends contrary to the Slater-Pauling curve, i.e., T_C increases with increasing $3d$ electron occupations. This contradiction is because those studies correlated the changes in T_C with those in the total $3d$ electron occupations.

Our microscopic study can explain the entangled mechanism of the electric field effect on T_C and the exchange interaction. In ultrathin magnetic films of Fe and Co, the exchange interaction between the d_{z^2} states is much smaller than the others because of a small overlap between the wave functions [51]. Therefore, in the present sample, states other than d_{z^2} dominate the magnetism. In particular, the electric-field-induced change in T_C is governed especially by the changes in the d_{xz} and d_{yz} states because of the relatively small changes in the $d_{x^2-y^2}$ and d_{xy} states.

The electric field application electrostatically injects/extracts charges into/from the Co surface, shifting the Fermi level. However, since the Fermi-level shift alone cannot explain the observed orbital-dependent changes by the electric field, we must consider another mechanism: electric field modifications of the orbital hybridizations, which have been verified theoretically [51–53] as well as, most recently, experimentally [54]. Indeed, the calculation part of Ref. [54] showed that, in a Pd/Co/Pt structure, the electric field modifications of the orbital hybridizations changes the electron occupations of the $5d$ states of Pt counter to the Fermi-level shift.

The d_{z^2} and $d_{xz(yz)}$ orbitals of Co at the Co/MgO interface can hybridize with the p_z and $p_{x(y)}$ orbitals of O in MgO, respectively. The slight extension (reduction) of the Co-O atomic distance by the negative (positive) electric field results in decreasing (increasing) the energy gap between the antibonding and bonding states formed by the hybridizations between the $3d$ orbitals of Co and the $2p$ orbitals of O [51].

Above all, the antibonding states of $d_{xz(yz)}$ are located near the Fermi level. They go up (down) by the positive (negative) electric field to decrease (increase) the occupied $d_{xz(yz)}$ states. The bonding and antibonding states formed by the orbital hybridization between the d_{z^2} and the p_z orbitals should be the most altered by the electric field. However, since the antibonding (bonding) states are located well above (below) the Fermi level, the electric field modification of the orbital hybridization between the d_{z^2} and the p_z orbitals can have a small impact on the electron occupation of the d_{z^2} states. Since the $d_{x^2-y^2}$ and d_{xy} orbitals do not hybridize with the $2p$ states of O, the electron occupations simply increase (decrease) by the positive (negative) electric field, i.e., $\Delta h_{d_{x^2-y^2}} + \Delta h_{d_{xy}} < 0$. Therefore, without assuming $\Delta h_{d_{x^2-y^2}} + \Delta h_{d_{xy}} \sim 0$ as above, we conclude that the electron occupations of the d_{xz} and d_{yz} states decrease (increase) by the positive (negative) electric field. It would be possible to discuss electric field effects on exchange stiffness in CoFeB/MgO structures [55,56] in the same manner. The positive electric field lowers the bonding states of $d_{xz(yz)}$, which are located near the Fermi level, to increase the occupied $d_{xz(yz)}$ states [51]. This is considered to result in the enhancement of exchange stiffness by the positive electric field.

We observed via the XAS and XMCD measurements the orbital-dependent changes of the electron occupations in the ultrathin Co-based on the sum rules. The positive electric field decreases the d_{z^2} holes but increases the $d_{xz(yz)}$ holes. The orbital-dependent changes of the electron occupations result from two competing mechanisms: the electric-field-induced shift of the Fermi level and changes in the orbital hybridizations. This variation of $d_{xz(yz)}$ states is considered to dominate the change in the T_C because of the much stronger exchange interactions in those states than in the d_{z^2} states.

We thank S. Kim, K.-J. Kim, M. Suzuki, and T. Moriyama for the fruitful discussions and Y. Hibino for offering us the CoO_x reference spectrum. This work was partly supported by JSPS KAKENHI (Grants No. 15H05702, No. 25220604, No. 26103002, No. 14J08822, No. 19H00860, and No. 16H05977), ImPACT Program of CSTI, Spintronics Research Network of Japan, and Collaborative Research Program of the Institute for Chemical Research, Kyoto University. The synchrotron radiation experiments were performed at SPring-8 with the approval of the Japan Synchrotron Radiation Research Institute (JASRI) (Proposals No. 2015B0902, No. 2016A0902, No. 2016B0117, and No. 2018A1225).

[1] Y. Tokura and N. Nagaosa, *Science* **288**, 462 (2000).
 [2] P. Bruno, *Phys. Rev. B* **39**, 865(R) (1989).
 [3] A. Manchon, H. C. Koo, J. Nitta, S. M. Frolov, and R. A. Duine, *Nat. Mater.* **14**, 871 (2015).
 [4] A. Soumyanarayanan, N. Reyren, A. Fert, and C. Panagopoulos, *Nature (London)* **539**, 509 (2016).
 [5] I. M. Miron, G. Gaudin, S. Auffret, B. Rodmacq, A. Schuhl, S. Pizzini, J. Vogel, and P. Gambardella, *Nat. Mater.* **9**, 230 (2010).
 [6] M. Bode, M. Heide, K. von Bergmann, P. Ferriani, S. Heinze, G. Bihlmayer, A. Kubetzka, O. Pietzsch, S. Blügel, and R. Wiesendanger, *Nature (London)* **447**, 190 (2007).

[7] G. Prenat, K. Jabeur, P. Vanhauwaert, G. D. Pendina, F. Oboril, R. Bishnoi, M. Ebrahimi, N. Lamard, O. Boulle, K. Garello, J. Langer, B. Ocker, M.-C. Cyrille, P. Gambardella, M. Tahoori, and G. Gaudin, *IEEE Trans. Multi-Scale Comput. Syst.* **2**, 49 (2016).
 [8] H. Ohno, D. Chiba, F. Matsukura, T. Omiya, E. Abe, T. Dietl, Y. Ohno, and K. Ohtani, *Nature (London)* **408**, 944 (2000).
 [9] F. Matsukura, Y. Tokura, and H. Ohno, *Nat. Nanotechnol.* **10**, 209 (2015).
 [10] M. Weisheit, S. Fähler, A. Marty, Y. Souche, C. Poinignon, and D. Givord, *Science* **315**, 349 (2007).

- [11] T. Maruyama, Y. Shiota, T. Nozaki, K. Ohta, N. Toda, M. Mizuguchi, A. A. Tulapurkar, T. Shinjo, M. Shiraishi, S. Mizukami, Y. Ando, and Y. Suzuki, *Nat. Nanotechnol.* **4**, 158 (2009).
- [12] K. Yamada, H. Kakaizaki, K. Shimamura, M. Kawaguchi, S. Fukami, N. Ishiwata, D. Chiba, and T. Ono, *Appl. Phys. Express* **6**, 073004 (2013).
- [13] D. Chiba, S. Fukami, K. Shimamura, N. Ishiwata, K. Kobayashi, and T. Ono, *Nat. Mater.* **10**, 853 (2011).
- [14] Y. Shiota, T. Nozaki, F. Bonell, S. Murakami, T. Shinjo, and Y. Suzuki, *Nat. Mater.* **11**, 39 (2012).
- [15] S. Kanai, M. Yamanouchi, S. Ikeda, Y. Nakatani, F. Matsukura, and H. Ohno, *Appl. Phys. Lett.* **101**, 122403 (2012).
- [16] T. Nozaki, T. Yamamoto, S. Miwa, M. Tsujikawa, M. Shirai, S. Yuasa, and Y. Suzuki, *Micromachines* **10**, 327 (2019).
- [17] J. Stöhr, *J. Magn. Magn. Mater.* **200**, 470 (1999).
- [18] G. van der Laan and A. I. Figueroa, *Coord. Chem. Rev.* **277-278**, 95 (2014).
- [19] Y. Wu, J. Stöhr, B. D. Hermsmeier, M. G. Samant, and D. Weller, *Phys. Rev. Lett.* **69**, 2307 (1992).
- [20] G. Y. Guo, H. Ebert, W. M. Temmerman, and P. J. Durham, *Phys. Rev. B* **50**, 3861 (1994).
- [21] B. T. Thole, P. Carra, F. Sette, and G. van der Laan, *Phys. Rev. Lett.* **68**, 1943 (1992).
- [22] P. Carra, B. T. Thole, M. Altarelli, and X. Wang, *Phys. Rev. Lett.* **70**, 694 (1993).
- [23] J. Stöhr and H. König, *Phys. Rev. Lett.* **75**, 3748 (1995).
- [24] A. Kohn *et al.*, *Appl. Phys. Lett.* **95**, 042506 (2009).
- [25] G. W. Watson, E. T. Kelsey, N. H. de Leeuw, D. J. Harris, and S. C. Parker, *J. Chem. Soc., Faraday Trans.* **92**, 433 (1996).
- [26] Th. Mühge, Th. Zeidler, Q. Wang, Ch. Morawe, N. Metoki, and H. Zabel, *J. Appl. Phys.* **77**, 1055 (1995).
- [27] See Supplemental Material at <http://link.aps.org/supplemental/10.1103/PhysRevB.102.100407> for further details of (1) the device fabrication process, (2) the electrical measurements, (3) the x-ray measurements, (4) the sum-rule analysis, (5) the analysis of the magnetic dipole moment, (6) the electric field modulation of magnetic anisotropy, (7) the verification of the existence of voltage-induced chemical reactions, and (8) reproducibility of electric-field-induced changes in the spectra, respectively.
- [28] A. Arrott, *Phys. Rev.* **108**, 1394 (1957).
- [29] F. Ando, K. T. Yamada, T. Koyama, M. Ishibashi, Y. Shiota, T. Moriyama, D. Chiba, and T. Ono, *Appl. Phys. Express* **11**, 073002 (2018).
- [30] M. Hashimoto, H. Qiu, T. Ohbuchi, M. Adamik, H. Nakai, A. Barna, and P. B. Barna, *J. Cryst. Growth* **166**, 792 (1996).
- [31] Y. Hibino, T. Koyama, A. Obinata, T. Hirai, S. Ota, K. Miwa, S. Ono, F. Matsukura, H. Ohno, and D. Chiba, *Appl. Phys. Lett.* **109**, 082403 (2016).
- [32] T. Nakamura, T. Muro, F. Z. Guo, T. Matsushita, T. Wakita, T. Hirono, Y. Takeuchi, and K. J. Kobayashi, *J. Electron. Spectrosc. Relat. Phenom.* **144-147**, 1035 (2005).
- [33] R. Nakajima, J. Stöhr, and Y. U. Idzerda, *Phys. Rev. B* **59**, 6421 (1999).
- [34] A. Obinata, T. Hirai, Y. Kotani, K. Toyoki, T. Nakamura, T. Koyama, and D. Chiba, *AIP Adv.* **8**, 115122 (2018).
- [35] Y. Hibino, T. Hirai, K. Hasegawa, T. Koyama, and D. Chiba, *Appl. Phys. Lett.* **111**, 132404 (2017).
- [36] F. Bonell, Y. T. Takahashi, D. D. Lam, S. Yoshida, Y. Shiota, S. Miwa, T. Nakamura, and Y. Suzuki, *Appl. Phys. Lett.* **102**, 152401 (2013).
- [37] C. Bi, Y. Liu, T. Newhouse-Illige, M. Xu, M. Rosales, J. W. Freeland, O. Mryasov, S. Zhang, S. G. E. te Velthuis, and W. G. Wang, *Phys. Rev. Lett.* **113**, 267202 (2014).
- [38] U. Bauer, L. Yao, A. J. Tan, P. Agrawal, S. Emori, H. L. Tuller, S. van Dijken, and G. S. D. Beach, *Nat. Mater.* **14**, 174 (2015).
- [39] Y. Wakabayashi, H. Fujii, T. Kimura, O. Sakata, H. Tajiri, T. Koyama, and D. Chiba, *Z. Phys. Chem.* **230**, 569 (2016).
- [40] G. van der Laan, *J. Phys.: Condens. Matter* **10**, 3239 (1998).
- [41] T. Oguchi and T. Shishidou, *Phys. Rev. B* **70**, 024412 (2004).
- [42] O. Šipr, J. Minár, and H. Ebert, *Phys. Rev. B* **94**, 144406 (2016).
- [43] S. Grytsyuk, A. Belabbes, P. M. Haney, H.-W. Lee, K.-J. Lee, M. D. Stiles, U. Schwingenschlögl, and A. Manchon, *Phys. Rev. B* **93**, 174421 (2016).
- [44] M. Tsujikawa, S. Haraguchi, T. Oda, Y. Miura, and M. Shirai, *J. Appl. Phys.* **109**, 07C107 (2011).
- [45] S. Miwa, M. Suzuki, M. Tsujikawa, K. Matsuda, T. Nozaki, K. Tanaka, T. Tsukahara, K. Nawaoka, M. Goto, Y. Kotani, T. Ohkubo, F. Bonell, E. Tamura, K. Hono, T. Nakamura, M. Shirai, S. Yuasa, and Y. Suzuki, *Nat. Commun.* **8**, 15848 (2017).
- [46] T. Kawabe, K. Yoshikawa, M. Tsujikawa, T. Tsukahara, K. Nawaoka, Y. Kotani, K. Toyoki, M. Goto, M. Suzuki, T. Nakamura, M. Shirai, Y. Suzuki, and S. Miwa, *Phys. Rev. B* **96**, 220412(R) (2017).
- [47] J. C. Slater, *Phys. Rev.* **49**, 931 (1936).
- [48] L. Pauling, *Phys. Rev.* **54**, 899 (1938).
- [49] C. Takahashi, M. Ogura, and H. Akai, *J. Phys.: Condens. Matter* **19**, 365233 (2007).
- [50] M. A. W. Schoen, J. Lucassen, H. T. Nembach, T. J. Silva, B. Koopmans, C. H. Back, and J. M. Shaw, *Phys. Rev. B* **95**, 134410 (2017).
- [51] A. M. Pradipto, T. Akiyama, T. Ito, and K. Nakamura, *Phys. Rev. B* **96**, 014425 (2017).
- [52] K. Nakamura, R. Shimabukuro, Y. Fujiwara, T. Akiyama, T. Ito, and A. J. Freeman, *Phys. Rev. Lett.* **102**, 187201 (2009).
- [53] M. Oba, K. Nakamura, T. Akiyama, T. Ito, M. Weinert, and A. J. Freeman, *Phys. Rev. Lett.* **114**, 107202 (2015).
- [54] K. T. Yamada, M. Suzuki, A.-M. Pradipto, T. Koyama, S. Kim, K.-J. Kim, S. Ono, T. Taniguchi, H. Mizuno, H. Ando, F. Oda, K. Kakizakai, H. Moriyama, K. Nakamura, D. Chiba, and T. Ono, *Phys. Rev. Lett.* **120**, 157203 (2018).
- [55] T. Dohi, S. Kanai, F. Matsukura, and H. Ohno, *AIP Adv.* **6**, 075017 (2016).
- [56] J. Cho, S. Miwa, K. Yakushiji, H. Kubota, A. Fukushima, C.-Y. You, S. Yuasa, and Y. Suzuki, *Phys. Rev. Appl.* **10**, 014033 (2018).